FERMILAB-PUB-75-183-E PRL

NUB 2262

July 7, 1975

# Measurement of $\psi$(3.1) Meson Production by Pions and Protons*

G. J. Blanar, C. F. Boyer, W. L. Faissler, D. A. Garelick†,
M. W. Gettner, M. J. Glaubman, J. R. Johnson, H. Johnstad,
M. L. Mallary, E. L. Pothier, D. M. Potter, M. T. Ronan,
M. F. Tautz, E. von Goeler, and Roy Weinstein

Northeastern University at Boston
Boston, Massachusetts 02115

* Supported in part by the National Science Foundation under grant MPS70-02059A5.

† Sloan Foundation Fellow.

## Abstract

The production of $\psi(3.1)$ mesons is reported for the reactions $\pi^- + Fe \rightarrow \mu^+ + \mu^- +$ anything, at 200 GeV, and $p + Fe \rightarrow \mu^+ + \mu^- +$ anything, at 240 GeV. For $\psi$ production, distributions in $x \equiv P_L/P_{Beam}$ and $P_\perp$ are given. For $x \geq 0.5$, the ratio of the $\psi$ production cross sections in iron for pions to that for protons is found to be $7.4 \pm 2.0$.

We report here results of an experiment carried out at the Fermi National Accelerator Laboratory, FNAL, in which enhancements are observed in the dimuon invariant mass spectra at about 3.1 GeV. The reactions studied were:

$$\pi^- + Fe \rightarrow \mu^+ + \mu^- + \text{anything} \quad ; \quad P_B = 200 \text{ GeV} \qquad (1)$$

and

$$p + Fe \rightarrow \mu^+ + \mu^- + \text{anything} \quad ; \quad P_B = 240 \text{ GeV} \qquad (2)$$

where $P_B$ is the monoenergetic beam momentum. We interpret the enhancements, whose widths are consistent with the resolution of our apparatus, as the $\psi(3.1)$ meson[1].

The $\mu$ pair detector is shown in Figure 1a. The $\mu$ pairs were created at the front end of the first iron (Fe) absorber. Muons were identified by their traversal of 5.6 m of Fe. Muon momenta and angles were measured using a 56 kGm gapless magnet and associated wire chamber system. Events were recorded whenever there was a six fold counter coincidence, M0·M1·(M2·M3)·(M4·M5), in time with a beam particle defined by scintillation counters and hodoscopes (not shown). The split counter coincidence, (M2·M3)·(M4·M5), required that there be at least two particles at the rear of the magnet. For each event, coordinates from the chambers, counter tags, and the pulse heights from counters MP1, MP2, M0, M1, two beam Cerenkov counters, and the final beam defining counter were recorded.

The dimuon invariant mass was calculated from the tracks measured by the spark chambers, assuming the dimuon was created inside the first Fe absorber 12.7 cm from its front edge along the beam line. The muon momenta and angles were reconstructed taking into account the bending and energy loss of the muons in the magnetized Fe spectrometer. The proportional

chamber was used only in checking the reconstruction technique and the spark chamber efficiencies for a subsample of the data.

The reconstruction process selected $\mu$ pairs for which the total charge was zero. This eliminated $\approx$ 2% of the $2\mu$ events. Also, in the horizontal plane projection, where there is no bending, each muon track was extrapolated back to the region of the production point. In this region, the tracks were required to deviate horizontally from the production point by less than 2.2 times the expected standard deviation. The standard deviation, $\Delta$, was calculated from the bending of the muon in the vertical plane (muon momentum) and the expected multiple scattering of the muon in the spectrometer. (At 100 GeV, $\Delta$ = 1 cm.) This requirement removed $\approx$ 10% of the events. For the accepted events, the distribution of track positions at the production point agreed well with the distribution calculated from the properties of the spectrometer. Monoenergetic muon beams with energies of approximately 100 and 200 GeV were used to calibrate and check the spectrometer and measure its resolution. Also, counters MP1 and MP2 were used to show that the contamination of the $\psi$ data from $\mu$ pairs produced upstream of the Fe is small and does not effect the results significantly. (A 60 cm hydrogen target was centered 60 cm upstream of the iron.)

The dimuon effective mass, $M_{\mu\mu}$, spectra observed in 45 hours of beam time are shown in Figs. 1(b) and 1(c). Only events which satisfied the reconstruction criteria discussed above and which had a total laboratory dimuon momentum, $P_L$, above 90 GeV are plotted. These data are not corrected for variation of spectrometer acceptance with mass. In the interval $2 \leq M_{\mu\mu} \leq 4$ GeV, the mass acceptance is a smooth structureless function of mass and varies by about $\pm$ 35%. The low mass regions of these spectra are presented as an indication of the overall $\mu$ pair spectrum and will be discussed elsewhere. The dashed curves drawn in the region $M_{\mu\mu} \approx 3$ GeV

represent the spectra calculated by a Monte Carlo method which takes into account the resolution and detection efficiency of the apparatus and assumes all of the events in the interval $2.5 \leq M_{\mu\mu} \leq 3.7$ GeV, the $\psi$ region, result from the decay $\psi \rightarrow \mu^+\mu^-$. In the $\psi$ regions, we observe 104 and 45 events in the pion and proton data, respectively. An extrapolation of the data with $M_{\mu\mu} < 2.5$ GeV into the $\psi$ regions indicates that the non $\psi$ contributions to the $\psi$ regions are less than 20%. Since the agreement between the dashed lines and the data is good[2], we interpret the observed enhancements as $\psi(3.1) \rightarrow \mu^+\mu^-$.

The acceptance corrected distributions in $x \equiv P_L/P_B$ and dimuon transverse momentum, $P_\perp$, are shown in Figures 2(a) and 2(b) for the $\psi$ region. (In calculating the geometric acceptance, isotropy for the decay $\psi \rightarrow \mu^+\mu^-$ was assumed.) The solid lines are fits to the measured cross sections of the form:

$$d^2\sigma/dxdP_\perp^2 \propto \exp(-ax - bP_\perp).$$

The results of the fits[3] are for incident pions $a_\pi = 6.2 \pm 0.8$ and $b_\pi = 1.6 \pm 0.2$ $(GeV)^{-1}$, and for incident protons $a_p = 9.7 \pm 1.6$ and $b_p = 2.2 \pm 0.5$ $(GeV)^{-1}$. We calculate that for both $\pi$'s and p's, the effect of $\psi$ production from secondaries produced in the Fe is negligible.

We have compared the yields of $\psi$ mesons per incident $\pi^-$, $Y_\pi$, to the yield per incident p, $Y_p$. The ratio of the yields, $R = Y_\pi/Y_p$, is x dependent. For $x \geq .5$, $R = 7.4 \pm 2.0$, where the quoted error in R is dominated by the statistical uncertainty in $Y_p$. Systematic uncertainties in R are estimated to be significantly less than the statistical uncertainties and have been neglected. The fact that R is significantly greater than unity, suggests

that the mechanisms for $\psi$ production at large x are basically different for $\pi$'s and p's. This difference may indicate that the antiquark in the $\pi^-$ plays a critical role in $\psi$ production.

For a total Fe inelastic cross section of $\sim$ .7 barns, our data give for $x \geq .5$ a total inclusive cross section for $\pi^-$ Fe $\rightarrow \psi \rightarrow \mu\mu$ of $\approx$ 85 nanobarns, $\pm$ 50%, where the error is dominated by systematic errors. Previous results for $\psi$ production by neutrons[4] of average energy 250 GeV from beryllium gave the probability per interacting neutron for nBe $\rightarrow \psi \rightarrow \mu\mu$, $|x| > .32$, as $P(n) = .43 \times 10^{-7}$ (quoted error of a factor of two). Our result for protons from Fe for $|x| \geq .38$ is $P(p) = (.59 \pm .30) \times 10^{-7}$ in reasonable agreement with the neutron result. The distributions in x and $P_\perp$ for the neutron data also appear consistent with our proton results.

We thank the Northeastern University Computation Center, the FNAL crew, and the FNAL Fabrication Procurement Group for their support, and Brookhaven National Laboratory and Harvard University for the loan of equipment. We also thank B. Cairns, E. King and D. Ronan for their help with this work.

## REFERENCES


1. J. J. Aubert et al., Phys. Rev. Lett. 33, 1404 (1975) and J. F. Augustin et al., Phys. Rev. Lett. 33, 1406 (1974).
2. If all $\psi$ production were via $\psi'(3.7)$ production only $7 \pm 4\%$ of the yield in the $\psi$ region of our data would be from $\psi'(3.7) \rightarrow \mu^+\mu^-$. This is based on the branching ratios from A. M. Boyarski et al., Phys. Rev. Lett. 34, 1357 (1975) and J. A. Kadyk et al., LBL report #3687 (unpublished).
3. Fits to $d^2\sigma/dxdP_\perp^2 \propto \exp(-b' P_\perp^2)$ give $b'_\pi = .81 \pm .14$ $(GeV)^{-2}$ and $b'_p = 1.1 \pm 0.3$ $(GeV)^{-2}$.
4. B. Knapp et al., Phys. Rev. Lett. 34, 1044 (1975).

## FIGURE CAPTIONS

Fig. 1 (a) Mu pair detector (top view). SC ≡ spark chamber; M ≡ scintillation counter; PC ≡ proportional chamber; SC2 limits the vertical aperture to $\pm$ 24 cm.

(b) - (c) Dimuon invariant mass spectra for reactions (1) (pion beam) and (2) (proton beam), respectively.

Fig. 2 (a) x distributions for pion and proton beams. For additional details, see text.

(b) $P_\perp$ distributions for pion and proton beams. For additional details, see text.

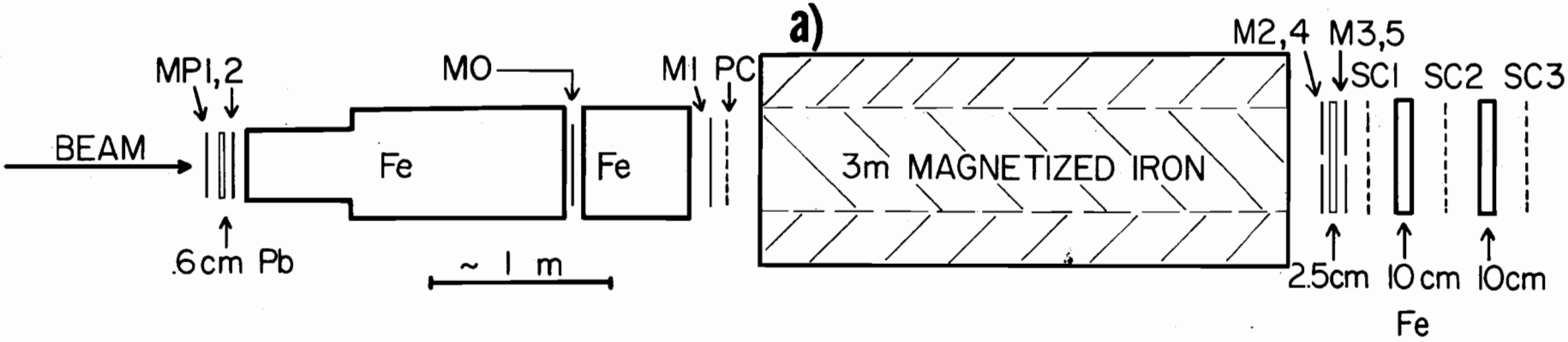
a)
MP1,2
MO
M1
PC
M2,4
M3,5
SC1
SC2
SC3
BEAM
Fe
Fe
3m MAGNETIZED IRON
.6cm Pb
~ 1 m
2.5cm
10 cm
10cm
Fe

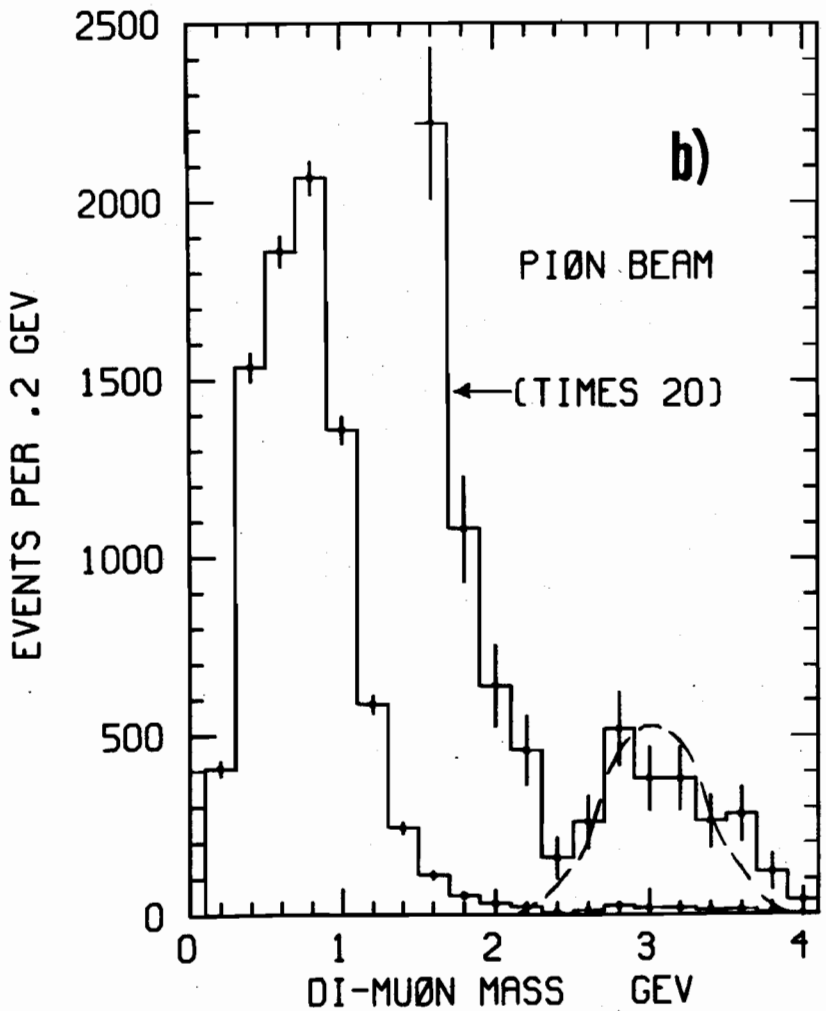
b)
PIØN BEAM
(TIMES 20)
EVENTS PER .2 GEV
DI-MUØN MASS GEV
0
500
1000
1500
2000
2500
0
1
2
3
4

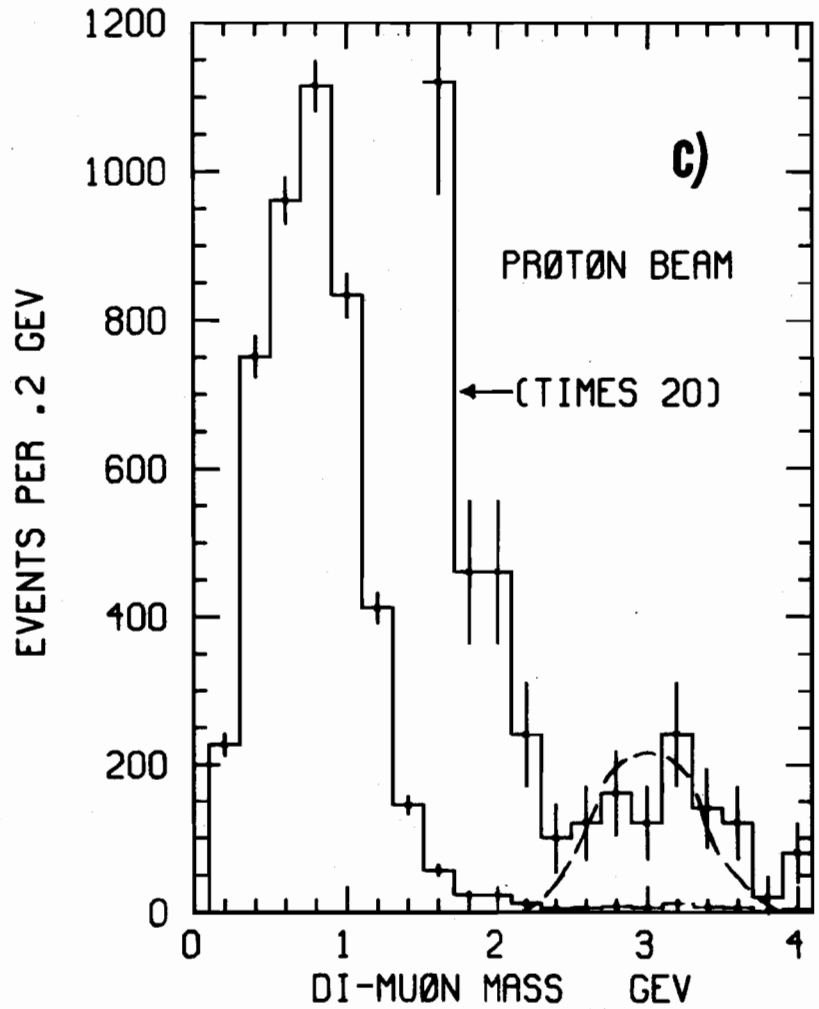
c)
PRØTØN BEAM
(TIMES 20)
EVENTS PER .2 GEV
DI-MUØN MASS GEV
0
200
400
600
800
1000
1200
0
1
2
3
4

Fig. 1

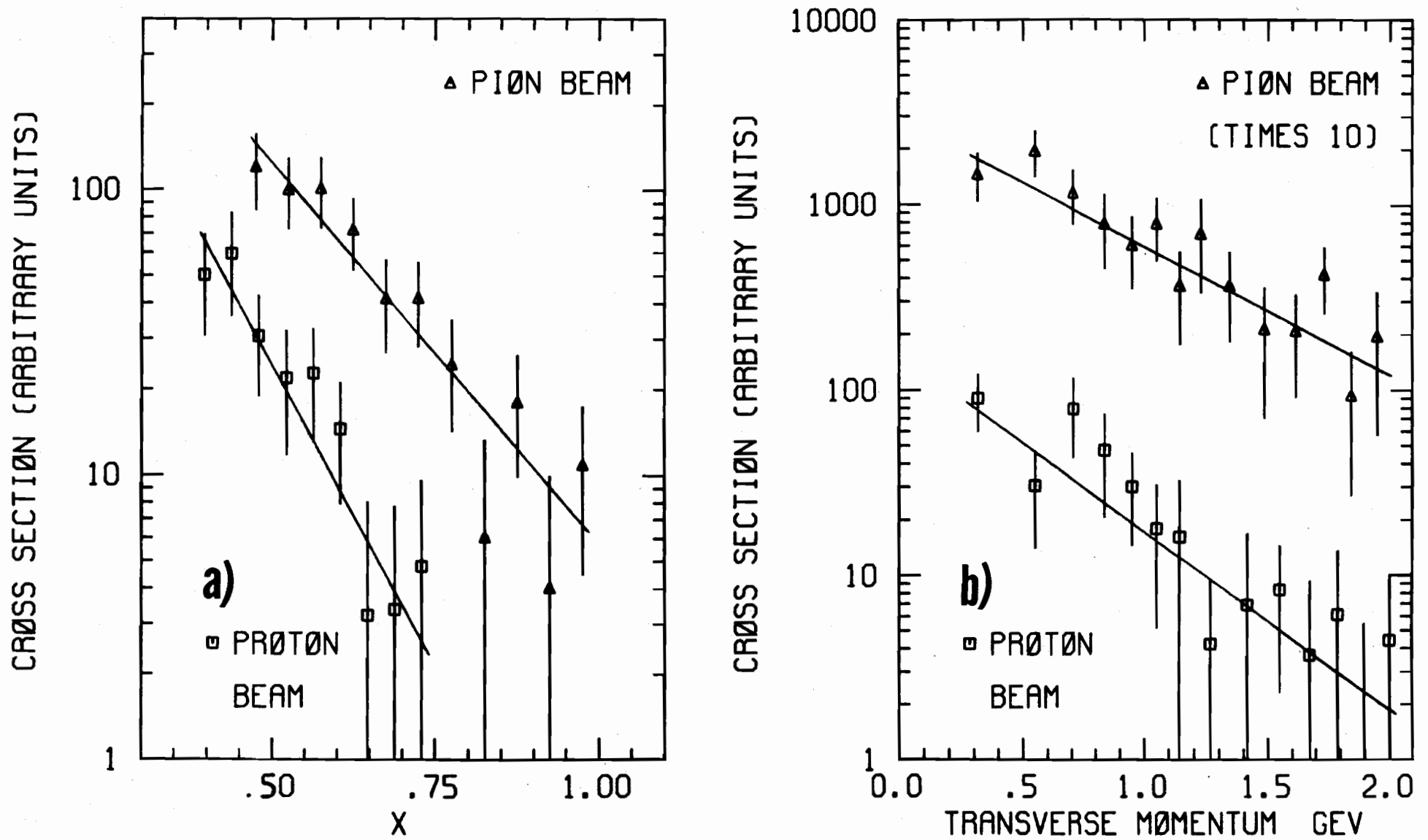
CRØSS SECTIØN (ARBITRARY UNITS)
100
10
1
PIØN BEAM
a)
PRØTØN
BEAM
.50
.75
1.00
X
10000
1000
100
10
1
PIØN BEAM
(TIMES 10)
b)
PRØTØN
BEAM
0.0
.5
1.0
1.5
2.0
TRANSVERSE MØMENTUM GEV

Fig. 2